

MOX–Report No. 28/2011

**Mathematical modelling for the evolution of aeolian
dunes formed by a mixture of sands:
entrainment-deposition formulation**

PISCHIUTTA, M.; FORMAGGIA, L.; NOBILE, F.

MOX, Dipartimento di Matematica “F. Brioschi”
Politecnico di Milano, Via Bonardi 9 - 20133 Milano (Italy)

mox@mate.polimi.it

<http://mox.polimi.it>

Mathematical modelling for the evolution of aeolian dunes formed by a mixture of sands: entrainment-deposition formulation

Matteo Pischiutta[‡], Luca Formaggia[‡], Fabio Nobile[‡]

June 22, 2011

[‡] MOX – Modellistica e Calcolo Scientifico
Dipartimento di Matematica “F. Brioschi”
Politecnico di Milano
via Bonardi 9, 20133 Milano, Italy
`matteo.pischiutta@mail.polimi.it`

Keywords: Sand dunes dynamics, entrainment-deposition formulation.

AMS Subject Classification: 76T25, 65Z05, 74F10.

Abstract

In this work we present a mathematical model of the evolution of aeolian sand dunes, in particular we consider the case of dunes formed by a mixture of sands with different characteristics. We first recall a basic model for the evolution of two dimensional sand dune that has been proposed in the literature. Then, we propose a novel type of mathematical formulation for the evolution of sand dunes formed by a mixture of two (or more) sands, which expresses the temporal variation of sand surface elevation and concentration of each sand type in terms of the balance between entrainment and deposition rates of sand. We provide some simple but physically based constitutive relationship for the new variables and we present some numerical simulations that clearly demonstrate that our model can be profitably adopted for the study of interesting physical problems such as sand tracking and dunes collision.

1 Introduction

The morphodynamics of sand dunes is due to two distinct physical mechanisms: the effect of the wind blowing on the sand surface which produces a flux of jumping sand grains called “in saltation”, and the spontaneous generation of avalanches if the slope of the sand surface is steeper than the angle of repose

of the sand. In the last decade the mathematical modelling and the numerical simulation of sand dune evolution has become an attractive topic in the aeolian literature. Starting from the fundamental works of H.Herrmann, K.Kroy and G.Sauermann [1, 2] which provide a minimal model for the evolution of two dimensional sand dunes, the successive developments have lead to realistic modelling and simulations of three dimensional transverse [3], barchans [4, 5] and linear [6] dunes, as well as the generation of complete dune fields [7]. In these works the mathematical model is often based on a conservation equation for the mass of sand formulated by balancing the temporal variation of sand surface elevation with the divergence of the saltation and avalanches sand fluxes.

In this paper, we are interested in building a model for dune evolution when the bulk sediment is a mixture of sands with different characteristics. In particular, here we consider the simplest case of sediments with different colours (tracer sediments), that has been studied *e.g.* in [8, 9] from an experimental point of view. To this aim, inspired by current approaches adopted in the fluvial literature [10], we assume that sediment exchange between sand surface and superficial transport flow is limited in a layer of finite depth commonly called *active layer*, and we build a complete model for differential sand dispersion coupled with sand surface evolution.

We show that this approach leads to a formulation for the conservation equation that links the temporal variation of sand surface elevation to the balance between entrainment and deposition rates [11]. We provide some constitutive relationship for the new variables introduced in the system: for the saltation flux, we write the entrainment rate in function of the shear stress exerted by the wind on the sand surface, while the deposition rate is linked to the upwind entrainment rate by assuming that the step length of a saltating grain is probabilistic with a given density function. For the avalanche flux, erosion occurs only if the slope exceeds the angle of repose; even in this case, we can introduce a probabilistic step length for avalanching grains which links the deposition rate to the up-slope entrainment rate. Furthermore, we are able to show that, under some simple but physically based hypothesis, the entrainment-deposition formulation for the evolution of two dimensional dunes is mathematically equivalent to the formulation based on the divergence of the sand flux to describe the evolution of an undifferentiated sand mass. However, the new formulation offers the possibility for a differential evolution of sand dunes made up of different sands.

The outline of the paper is the following: in Section 2 we recall the essential features of the classical model, detailing the type of discretization that we adopted for the numerical simulation. In Section 3, we formulate the model for marked sand dispersion during dune evolution, then we introduce the entrainment-deposition formulation, showing its consistency with the previous model. Finally, we present some numerical simulations which demonstrates that the model provides physically sound results.

2 Sand transport and desert surface evolution

The geometry of the system is represented in Figure 1, where the sand surface elevation is described by a function $z = h(x, t)$, z being the vertical coordinate. For simplicity we consider the evolution of a two-dimensional dune only. The evolution of the sand surface is due to the mass sand flux $q(x, t)$ of sand grain in saltation, that is the mass of sand that crosses the position x per unit time.

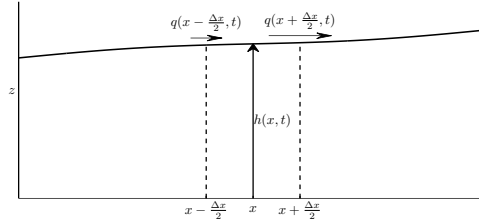


Figure 1: Geometry of the system; the temporal variation of the elevation of the sand surface $\partial_t h$ is due to divergence of the sand flux $\partial_x q$.

The continuity equation which ensures mass conservation is

$$\rho_{dune} \frac{\partial h}{\partial t} + \frac{\partial q}{\partial x} = 0, \quad (1)$$

where ρ_{dune} is the density of the sand bed given by $\rho_{dune} = (1 - \lambda)\rho_{sand}$, where λ is the porosity of sand bed, here assumed constant. We need to express the flux $q(x, t)$ in terms of the height profile $h(x, t)$ and the action of external wind. Since the speed of evolution of the surface is very small compared to that of sand transport, the topography can be assumed to be stationary with respect to the wind and sand transport dynamics. This assumption allows us to calculate the flux $q(x)$ by the following steps:

1. calculate the stationary wind velocity above the given topography; more precisely we need the shear velocity $u_* = u_*(x)$ or equivalently the shear stress $\tau = \rho_{air} u_*^2$ exerted by the wind on the sand surface;
2. calculate the stationary sand flux $q(x)$ for a given $\tau(x)$.

2.1 Shear stress calculation

The determination of the shear stress $\tau(x)$ is a rather complex problem due to the complex fluid dynamics in the atmospheric boundary layer in presence of saltating sand grains, and to the possible presence of a recirculation zone in the downwind part of a dune profile. In the areas not interested by recirculation we assume that the presence of the relief $h(x)$ induces a perturbation of the shear stress exerted by the wind with respect to that of a horizontal surface

$\tau_0 = \rho_{air} U_*$. We introduce then $\hat{\tau}(x) \equiv \tau(x)/\tau_0 - 1$, and we first consider the case of a smooth sand bump without recirculating zone. The analytic theory of boundary layer perturbation developed by P.S.Jackson and J.C.R.Hunt [12] and simplified for the sand dune problem by K.Kroy *et al.* [1], gives the following expression:

$$\hat{\tau}(x) = A \int_{\mathbb{R}} \frac{1}{\pi\chi} \partial_x h(x - \chi) d\chi + B \partial_x h(x) = \hat{\tau}_A + \hat{\tau}_B. \quad (2)$$

The shear stress perturbation $\hat{\tau}$ depends only on the slope of the hill $\partial_x h$, reflecting the consideration that a turbulent flux is scale-invariant. The convolution integral is a non local term that depends on the whole shape of the dune. Its contribution is positive on bumps (negative curvature) and negative on hollows (positive curvature). The second term takes into account the slope effects, as the shear stress increases on positive slopes because of streamline compression. The combined effects of these two contributions leads to an asymmetric shear stress even on a symmetric sand surface profile; in particular, the maximum of $\tau(x)$ is always shifted upwind with respect to the maximum of $h(x)$, see Figure 2(a). The value of the coefficients A and B is found in the cited literature [1].

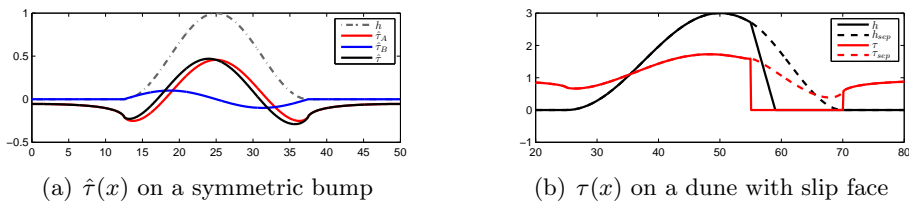


Figure 2: In (a), in black is represented the shear stress perturbation $\hat{\tau}$ on the profile h ; in red $\hat{\tau}_A$, the non-local term expressed by the convolution integral, in blue the slope term $\hat{\tau}_B$. The values of the parameters are $A = 4$, $B = 1$. In (b), in black is represented the dune profile h ; from the brink point, the separating streamline (dashed black line) is empirically built as a polynomial of 3rd degree. Then the shear stress (dashed red line) is calculated using Equation (2) on the profile which includes the separating streamline, and finally it is set to zero in the recirculating zone (red line).

In the case of the atmospheric boundary layer, the scale invariance is broken by the existence of the superficial roughness z_0 , and the coefficients A and B of the model are not strictly constant but depend on $\log(D/z_0)$, where D is the dune size. Notwithstanding, taking the coefficients as effective constant will not affect the overall behaviour of the model; further consideration in this direction can be found in [13, 14].

When the sand surface presents a slip face the wind flow separates at the brink of the dune and reattaches downwind. This phenomenon creates a recirculating

zone in the lee side of the dune, which cannot be modelled by the analytical perturbation method. A simple way to model the effect of the recirculation bubble on the overall flux is to empirically reconstruct the separating streamline and to assume that the wind flow follows it as a solid surface. In the recirculation zone the shear stress is then assumed to be negligible, see Figure 2(b). Following [2, 14], the separation streamline is written as a polynomial of 3rd degree with smooth C^1 junction at brink and reattachment point. The length of the separation bubble is determined by imposing the fixed maximum slope of $\tan 14^\circ$ at the inflexion point.

This extremely simplified method for shear stress calculation can reproduce the overall behaviour of the wind flux over a sand dune, saving a lot of computational time with respect to other methods. Since computing the shear stress by a CFD code is rather expensive, in the following we will use the proposed analytical expression for the shear stress.

2.2 Sand flux calculation

Wind blowing over a surface covered by sand mobilizes sand grains laying on the surface. Those grains accelerate extracting momentum from the wind flow and entrain other grains when they impact on the sand bed. In this process, the wind velocity in the surface layer is reduced. This feedback mechanism establishes a relation between the shear velocity u_* and the sand flux q at equilibrium. A single empirical relation has been proposed by R.A.Bagnold [15]:

$$q_{sat} = C \frac{\rho_{air}}{g} u_*^3, \quad (3)$$

where the index *sat* in Equation (3) emphasizes that this relation is valid when the flux is saturated, *i.e.* it is equal to its equilibrium transport capacity. Here C is a constant parameter usually taken equal to 2, ρ_{air} is the density of the air and g is the gravity acceleration. Many other laws have been discussed in the literature, mainly to include a threshold value for the shear velocity u_{th} in the formulation, indicating that below u_{th} the wind cannot mobilize the sand grains, but the scaling $q_{sat} \propto u_*^3$ is common to all models for u_* sufficiently far from the threshold value.

In field conditions not all the ground is covered by sand, moreover we have the presence of sloped beds and reattachment points. Therefore q_{sat} depends on x because $u_* = u_*(x)$, and the sand flux q is not everywhere equal to its saturated value given in Equation (3). In fact, the flux adapts to changes in external conditions with a characteristic space lag, called saturation length L_{sat} . This space lag can be described [14] by a charge equation of the form:

$$\frac{\partial q}{\partial x} = \frac{q_{sat} - q}{L_{sat}}. \quad (4)$$

This equation is valid only if some grains are available on the unerodible bed, *i.e.* if $h(x) > 0$. On the firm soil the flux cannot increase to become saturated

and remains constant.

Among the possible physical mechanisms responsible for the saturation length proposed in the literature, the most accredited is the distance required by the wind to accelerate the grain expelled from the surface and the value of this distance is taken proportional to the diameter of the grain times the ratio between the density of sand and air [13]: $L_{sat} = \xi \frac{\rho_{sand}}{\rho_{air}} d$. The value of the constant of proportionality $\xi \simeq 2$ was obtained recently [16] by adapting the charge equation (4) to experimental measurements conducted in a wind tunnel and appears to be independent from the strength of the wind. Characteristic values are $\rho_{sand} = 2650\text{kg/m}^3$, $\rho_{air} = 1.225\text{kg/m}^3$, $d = 0.25\text{mm}$, which lead to $L_{sat} = 1\text{m}$. The spatial delay between shear stress and sand flux profiles due to the saturation length introduce a length scale responsible for the existence of a minimal size for the sand dune: a too small bump of sand is in fact always eroded, see Figure 3.

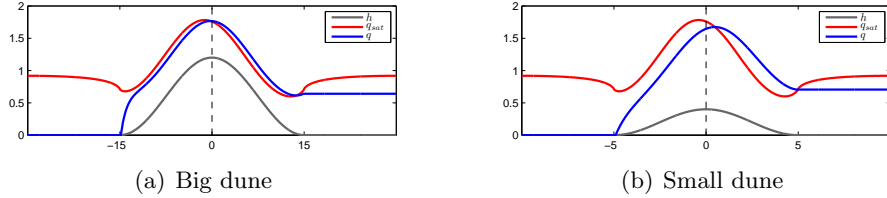


Figure 3: The effect of the saturation length; on two scale invariant surface profile (in grey), the profile of the saturated sand flux (in red) is equivalent (since the shear stress is scale invariant), but the saturation length add a spatial delay which makes the evolution of a big dune (a) possible ($q(x)$ and $h(x)$ have a maximum at the same position) but is responsible for the complete erosion of the small sand dune (b) ($q(x)$ has a maximum shifted in the downwind part of the dune).

2.3 Numerical simulation

The basic mathematical model for sand dune evolution is finally formed by the following equations:

$$\left\{ \begin{array}{l} \rho_{dune} \frac{\partial h}{\partial t} + \frac{\partial q}{\partial x} = 0 \quad \text{s.t.} \quad |\partial_x h| < \tan \gamma \\ \frac{u_*^2(x)}{U_*^2} = \frac{\tau(x)}{\tau_0} = 1 + A \int \frac{1}{\pi \chi} \partial_x h(x - \chi) d\chi + B \partial_x h(x) \\ q_{sat}(x) = C_B \frac{\rho_{air}}{g} u_*^3(x) \\ \frac{\partial q}{\partial x} = \frac{q_{sat} - q}{L_{sat}} \quad \text{where} \quad h > 0, \quad \frac{\partial q}{\partial x} = 0 \quad \text{otherwise,} \end{array} \right. \quad (5)$$

where in the first equation we impose that the slope of the sand surface cannot exceed the angle of repose during evolution. A typical value of γ is 34° . Concerning the numerical solution of (5), an initial profile $h(x, 0)$ is imposed and the domain $\Omega = [0, L]$ is divided in N intervals of uniform length Δx . The algorithm for the evolution of the system reads:

1. if the sand surface presents a slip face, then reconstruct the separating streamline using a 3rd order polynomial starting from the brink and reattaching downwind with a C^1 junction. The reattachment point is determined by imposing a slope at the inflection point of the streamline equal to $\tan 14^\circ$, following [1, 14].
2. Solve the equation for $\tau(x)$, which has an equivalent formulation using Fourier transform:

$$\begin{aligned}\mathcal{F}(\hat{\tau})(k) &= (A|k| + Bik)\mathcal{F}(h)(k), \\ \tau(x) &= \tau_0(1 + \hat{\tau}(x)).\end{aligned}$$

We use a Fast Fourier Transform, where h is the profile which eventually includes the separating streamlines. Then set $\tau = 0$ in the recirculating zones and deduce the profile of $q_{sat}(x)$ from the profile of $\tau(x)$.

3. The charge equation for $q(x)$ is an ODE in space which is solved with the Heun method (2nd order accurate explicit).
4. The time evolution of the surface is discretized with a forward Euler method and a WENO [17] reconstruction for $\partial_x q$, as we want to limit oscillation induced by a numerical differentiation of the profile of $q(x)$, which is only C^0 at the brink points. The profile obtained at this stage is indicated as $h^{n+1/2}$.
5. The suffix $n + 1/2$ is used to indicate that surface thus obtained is an intermediate solution as we still have to impose the constraint on the norm of the gradient. The solution that we adopted for this problem is detailed in Section 2.4.

The model can be applied to the evolution of an initial symmetric profile of sand to a moving dune with slip face as represented in Figure 4.

2.4 Algorithm for the constrained evolution

Following A.Caboussat & R.Glowinski [18], the problem of satisfying the constraint on the norm of the gradient is formulated as a variational inequality, and solved with the following augmented Lagrangian method. Let $V = H^1(\Omega)$ and, to ease notation, let $f = h^{n+1/2}$ be the intermediate solution. At each time iteration we want to find:

$$h^{n+1} = \arg \min_{v \in K} \frac{1}{2} \int_{\Omega} |v - f|^2 dx,$$

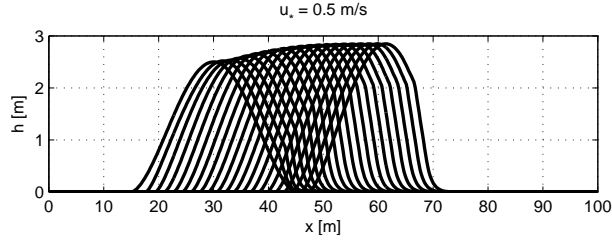


Figure 4: Evolution of an initial symmetric sand bump to a dune with slip face.

where $K = \{v \in V : |\partial_x v| \leq \tan \gamma\}$. To this aim we use a penalization technique

$$h^{n+1} = \arg \min_{v \in V} \frac{1}{2} \int_{\Omega} |v|^2 dx - \int_{\Omega} f v dx + \frac{1}{3\varepsilon} \int_{\Omega} \left((|\nabla v|^2 - \gamma^2)^+ \right)^3 dx,$$

where ε is a very small penalization parameter. Let us introduce $q = \nabla v \in L^2(\Omega)$ and denote $L^2(\Omega)$ by Q ; the problem is therefore equivalent to find:

$$\min_{\{v, q\} \in \mathcal{K}} \frac{1}{2} \int_{\Omega} |v|^2 dx - \int_{\Omega} f v dx + \frac{1}{3\varepsilon} \int_{\Omega} \left((|q|^2 - \gamma^2)^+ \right)^3 dx,$$

where

$$\mathcal{K} = \{(v, q) \in V \times Q : \nabla v - q = 0\}.$$

The relation $\nabla v - q = 0$ is imposed by penalization and the use of a Lagrangian multiplier $\mu \in Q$, defining the augmented Lagrangian functional:

$$\begin{aligned} \mathcal{L}_r(v, q, \mu) &= \frac{1}{2} \int_{\Omega} |v|^2 dx + \frac{r}{2} \int_{\Omega} |\nabla v - q|^2 dx + \int_{\Omega} \mu \cdot (\nabla v - q) dx \\ &\quad - \int_{\Omega} f v dx + \frac{1}{3\varepsilon} \int_{\Omega} \left((|q|^2 - \gamma^2)^+ \right)^3 dx. \end{aligned}$$

The corresponding saddle point problem is solved by using finite elements (piecewise linear for the approximation of V , piecewise constant for Q) and an Uzawa-type algorithm.

3 Marked sand dispersion

We are now interested in building a mathematical model for the dispersion of a mass of marked sand. The question we want to answer is: if we put a mass of sand grains that we can distinguish from the others in a zone of the sedimentary column interested in dune movement, how the concentration of marked grains in the sedimentary column will evolve?

3.1 The active layer setting

Due to the lack of literature on this specific topic in the aeolian framework, we directed our attention to the fluvial literature. In this field it is often necessary to formulate sediment transport models considering the variety of granulometric classes which composes the river bed. We extended the *active layer* framework (see *e.g.* G.Parker, [10]) to our problem. More precisely, we consider the mass balance for marked sand in a vertical column of infinitesimal width as

$$\rho_{dune} \frac{\partial}{\partial t} \left[\int_0^{h(t)} \tilde{f} dz \right] + \frac{\partial \tilde{q}}{\partial x} = 0, \quad (6)$$

where $\tilde{f}(x, z, t)$ is the fraction of marked sand at point (x, z) of the sedimentary column and $\tilde{q}(x, t)$ is the mass flux of the marked sand. The following hypothesis are added, see Fig. 5:

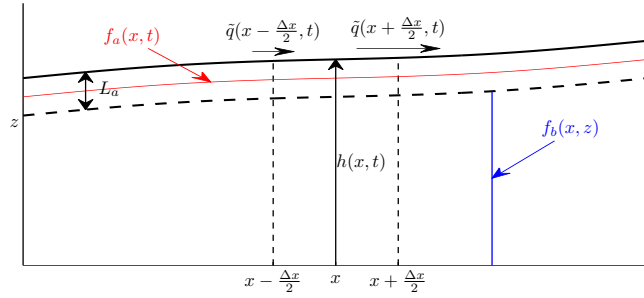


Figure 5: The active layer framework: in the active layer, the marked sand concentration $f_a(x, t)$ does not depend on the vertical coordinate z ; in the substrate, the marked sand concentration $f_b(x, z)$ does not change in time.

1. sediments being transported exchange mass with bed sediment only in a superficial layer of finite thickness L_a , named *active layer*;
2. the active layer is well mixed by the exchange process so that it has no vertical structure, therefore we can define:

$$\tilde{f}(x, z, t) = f_a(x, t) \quad \text{if} \quad h - L_a < z < h;$$

3. the substrate can have a vertical structure, and thus a functional dependence in z , but it does not change in time because it is below the zone that is transported:

$$\tilde{f}(x, z, t) = f_b(x, z) \quad \text{if} \quad z < h - L_a.$$

These hypotheses allow us to write Equation (6) separately for the active layer and the substrate:

$$\rho_{dune} \frac{\partial}{\partial t} \left[\int_{h(t)-L_a}^{h(t)} f_a(x, t) dz \right] + \Phi + \frac{\partial \tilde{q}}{\partial x} = 0 \quad (7)$$

$$\rho_{dune} \frac{\partial}{\partial t} \left[\int_0^{h(t)-L_a} f_b(x, z) dz \right] - \Phi = 0, \quad (8)$$

where the new term $\Phi(x, t)$ is the mass rate of marked sand through the internal surface $z = h(x, t) - L_a$ separating the active layer and the substrate. If the sand surface is locally in erosion ($\partial_t h < 0$), the active layer incorporates sediments from the substrate, and the interface mass rate will be $\Phi = \rho_{dune} f_b|_{z=h-L_a} \partial_t (h - L_a)$. Otherwise, if the sand surface is locally in deposition ($\partial_t h > 0$), the active layer passes sediments to the substrate, and the interface mass rate will be $\Phi = \rho_{dune} f_a \partial_t (h - L_a)$. These considerations can be incorporated in the definition of the interface concentration:

$$f_I = \begin{cases} f_b|_{z=h-L_a} & \text{if } \partial_t h < 0, \\ f_a & \text{if } \partial_t h > 0, \end{cases} \quad (9)$$

which allows us to write Equation (7) in the compact form:

$$\rho_{dune} \left[\frac{\partial(L_a f_a)}{\partial t} + f_I \frac{\partial(h - L_a)}{\partial t} \right] + \frac{\partial \tilde{q}}{\partial x} = 0. \quad (10)$$

Equation(10) is the conservation equation for marked sand in the active layer, and describes the evolution of the surface concentration of marked sand when sand is transported.

To close the system, we still have to characterize the new variables. In fluvial literature, L_a is assumed to be proportional to the diameter of bed sediments, yet since we consider uniform sediments we can take L_a as an effective parameter, which, by considering also Equation (1), leads to write Equation (10) as:

$$\rho_{dune} L_a \frac{\partial f_a}{\partial t} - f_I \frac{\partial q}{\partial x} + \frac{\partial \tilde{q}}{\partial x} = 0. \quad (11)$$

At this point, we need an expression for the divergence of the flux of marked sand $\partial_x \tilde{q}$. This term is equal to the balance between the entrainment and deposition rates of marked sand,

$$\frac{\partial \tilde{q}}{\partial x} = \tilde{E}(x) - \tilde{D}(x), \quad (12)$$

where $\tilde{E}(x)$ is the mass of marked sand that leaves a unit surface in the unit time to enter in the saltation flux and $\tilde{D}(x)$ is, conversely, the mass of marked sand that leaves the saltation flux and is deposited on the sand surface. In the next section we will provide some possible constitutive relationship for these rates.

3.2 Entrainment-deposition formulation

Let us come back to the total mass balance equation (1), which does not distinguish between marked and unmarked sand. It is however possible to replace the divergence of the sand flux with the balance between the total entrainment and deposition rates (respectively $E = E(x, t)$ and $D = D(x, t)$),

$$\frac{\partial q}{\partial x} = E - D, \quad (13)$$

so that the mass balance equation (1) will take the form:

$$\rho_{dune} \frac{\partial h}{\partial t} = D - E. \quad (14)$$

Because the time scale of transport dynamics is well separated from that of the evolution of the sand surface, it is possible to adopt a quasi-static formulation and assume that E and D adapt instantaneously to the changes of $h(x, t)$. To determine the relation linking the deposition to the entrainment we further assume that [11, 19]:

1. once entrained from the sand surface, a sand grain performs a step (eventually rebounding) of length r before depositing again on the surface;
2. the step length is probabilistic, with probability density function (p.d.f) $s(r)$, with $r \in (0, +\infty)$.

With these hypotheses we may write that

$$D(x) = \int_{-\infty}^x E(y)s(x-y) dy = \int_0^{+\infty} E(x-y)s(y) dy. \quad (15)$$

Now, the problem is switched to the characterization of the entrainment rate and the p.d.f. for step length. We should first point out that, to the best of our knowledge, this entrainment-deposition formulation has not yet been proposed in the aeolian literature; consequently, the problem of the characterization of the entrainment rate and the p.d.f. of step length have not yet been investigated, either from the theoretical, or from the experimental point of view.

Since the focus of this communication is on the formulation of a mathematical model of marked sand dispersion, we limit ourselves to propose an entrainment-deposition formulation that is consistent with the minimal model for sand dune evolution exposed in Section 2.

We first recall a useful relation that links the entrainment rate and the sand flux:

Proposition 3.1 *Let $\lambda = \int_0^{+\infty} rs(r) dr < \infty$ be the mean step length. We suppose that $q(0) = 0$ and consider a constant entrainment rate on the positive axis. Then, the saturated entrainment rate E_{sat} that leads to a saturated flux q_{sat} is*

$$E_{sat} = \frac{q_{sat}}{\lambda}.$$

Proof. We can define $q_{sat} = \lim_{x \rightarrow +\infty} q(x)$. Hence we can write

$$\begin{aligned} q(x) &= \int_0^x \frac{\partial q}{\partial y} dy = \int_0^x (E(y) - D(y)) dy = \\ &= \int_0^x \left(E(y) - \int_0^y E(y-z)s(z) dz \right) dy = \\ &= E_{sat} \int_0^x \left(1 - \int_0^y s(z) dz \right) dy = \\ &= E_{sat} \left[\left(\int_x^{+\infty} s(z) dz \right) x + \int_0^x s(y)y dy \right], \end{aligned}$$

and when $x \rightarrow +\infty$ the first term vanishes and the second one is equal to the mean step length λ . \square

We now use this relation to propose a constitutive model consistent with the one based on the sand flux formulation (3)-(4):

Proposition 3.2 *If we suppose that:*

1. *the entrainment rate is always equal to its saturated value:*

$$E(x) = \frac{q_{sat}(x)}{\lambda} \quad (16)$$

2. *the probability density function for the step length is exponential:*

$$s(r) = \frac{1}{\lambda} e^{-\frac{r}{\lambda}} \quad (17)$$

then the entrainment-deposition formulation is equivalent to the linear charge equation for the sand flux (4) with $L_{sat} = \lambda$.

Proof. It suffices to note that the solution of the charge equation (4), for example with the boundary condition $q(-\infty) = 0$, is

$$q(x) = \int_{-\infty}^x q_{sat}(y) \frac{1}{L_{sat}} e^{-\frac{x-y}{L_{sat}}} dy.$$

Thus the convolution with an exponential is naturally embedded in the analytical solution of the linear charge equation. The equivalence between the two formulation is therefore assessed by recognizing that, using the given hypothesis,

$$\begin{aligned} \frac{\partial q}{\partial x} &= E(x) - D(x) = \frac{q_{sat}(x)}{\lambda} - \int_{-\infty}^x \frac{q_{sat}(y)}{\lambda} \frac{1}{\lambda} e^{-\frac{x-y}{\lambda}} dy \\ &= \frac{q_{sat}(x) - q(x)}{\lambda}. \end{aligned}$$

\square

The proposed formulation reproduces the effect of saturation of the sand flux thanks to the space lag existing between the phenomena of erosion and deposition, predicting a saturation length equal to the mean step length for sand

grains. In Section 2.2 we reported that in the aeolian literature the saturation length is often assumed equal to 1m. This value seems to be compatible with the mean step length of a sand grain (remember that the step may include several rebounds), hence this value will be assumed as effective parameter in our model.

3.3 Application to the marked sand dispersion problem

We can now go back to the problem of marked sand dispersion. In equation (12) we decided to substitute the divergence of the sand flux of marked sediment with the imbalance between entrainment \tilde{E} and deposition rates \tilde{D} of marked sand. Once the total entrainment rate is known, the active layer hypothesis leads naturally to the following expressions for \tilde{E} and \tilde{D} :

$$\tilde{E}(x) = f_a(x)E(x), \quad \tilde{D}(x) = \int_{-\infty}^x f_a(y)E(y)s(x-y) dy. \quad (18)$$

In the new setting, equation (11) is conveniently rewritten in the form:

$$\rho_{dune}L_a \frac{\partial f_a}{\partial t} = \tilde{D} - \tilde{E} - f_I(D - E), \quad (19)$$

where the left hand side represents the temporal variation of mass of marked sand in the active layer, which is due on the one hand to the imbalance between entrainment and deposition superficial rates of marked sand ($\tilde{D} - \tilde{E}$) and on the other hand to the amount of mass of marked sand which leaves (enter) the active layer at the interface with the substrate if net deposition (erosion) locally occurs. In addition, the evolution of the substrate concentration is governed by Equation (8) which we conveniently rewrite in equivalent form here below. The complete system of equations which compose the model of marked sand dispersion during sand surface evolution finally reads:

$$\left\{ \begin{array}{l} \frac{u_*^2(x)}{U_*^2} = \frac{\tau(x)}{\tau_0} = 1 + A \int \frac{1}{\pi\chi} \partial_x h(x-\chi) d\chi + B \partial_x h(x) \\ \left\{ \begin{array}{l} E(x) = C_B \frac{\rho_{air}}{g} \frac{u_*^3(x)}{\lambda}, \quad D(x) = \int_{-\infty}^x E(y)s(x-y) dy \\ \rho_{dune} \frac{\partial h}{\partial t} = D - E \quad \text{s.t.} \quad |\partial_x h| < \tan \gamma, \end{array} \right. \\ \left\{ \begin{array}{l} \tilde{E}(x) = E(x)f_a(x) \quad \tilde{D}(x) = \int_{-\infty}^x E(y)f_a(y)s(x-y) dy \\ \rho_{dune}L_a \frac{\partial f_a}{\partial t} = \tilde{D} - \tilde{E} - f_I(D - E) \\ f_b(x, h(x, t) - L_a) = f_a(x, t) \quad \text{if} \quad z < h(x, t) - L_a. \end{array} \right. \end{array} \right. \quad (20)$$

In the zone characterized by net deposition of sediments, the substrate incorporates sediments from the active layer, so that we need a storage technique for the marked sand concentration in the sedimentary column during evolution. This will be discussed in section 3.5. First we need to provide a model for sand avalanches able to describe the dispersion of marked sand.

3.4 Description of avalanches

Besides the sand in saltation, the other transport mechanism is due to avalanches that spontaneously arise if the local slope exceeds the angle of repose of sand. In the first part of this paper we have treated sand avalanches as an instantaneous event which acts as a constraint on the maximum slope of the sand surface. This approach is profitable since we can avoid the accurate description of the avalanche process. On the other hand with this approach it is not possible to obtain a model for the transport of marked sand, so we need to derive an alternative formulation.

We propose to describe also the avalanche process using an entrainment-deposition formulation; we write therefore the following balance equation for the avalanche process (assuming that no saltation flux is present in the region affected by avalanches):

$$\rho_{dune} \frac{\partial h}{\partial t} = D_{av} - E_{av}. \quad (21)$$

In avalanches the sand begins to move when the local slope exceeds the angle of repose; we then assume the entrainment rate to be proportional to the excess of local slope with respect to the angle of repose:

$$E_{av}(x) = M \max(|\partial_x h(x)| - \tan \gamma, 0), \quad (22)$$

where M is a parameter whose dimensions are Kg/m²s. Again, we can suppose that the entrained sand is deposited along the slip face after rolling for a distance r . As in the case of sand in saltation, we can assume that this distance is probabilistic with p.d.f. $s_{av}(r)$, and link the deposit to what is entrained above through an integral relation:

$$D_{av}(x) = \int_{x_B}^x E_{av}(y) s_{av}(x - y) dy, \quad (23)$$

where x_B is the position of the brink of the slip face. In practical application both avalanches and saltation are present. The time scales of avalanches are much smaller than the time scales of saltation, implying that the constant M is large. So in practice we iterate Equation (21) until convergence is reached before considering the evolution given by the saltation flux.

3.5 Numerical simulations

In this section we detail the discretization techniques that we adopted for the numerical resolution of the mathematical models proposed in the previous sections. At the same time, we illustrate some numerical simulations, aiming at showing the potential fields of application of our research.

In the following, we will always consider a domain $x \in [0, L]$ subdivided in N_x intervals of equal size $\Delta x = L/N_x$. The midpoints $x_i = (i - 0.5)\Delta x$, $i = 1, \dots, N_x$ are the point where the variables are approximated using the standard notation

$f_i \simeq f(x_i)$ and the vectors $\mathbf{f} : [\mathbf{f}]_i = f_i$ are the unknowns of the problem. All the time derivatives are discretized with forward Euler method, and the deposition rate is computed by integrating the second integral in (15) by a trapezoidal rule. Concerning the numerical discretization in time of the marked sand dispersion model, the evolutionary equations for the sand surface and for the active layer concentration are discretized with forward Euler method with the same time step:

$$\begin{cases} \mathbf{h}^{n+1} &= \mathbf{h}^n + \frac{\Delta t}{\rho_{sand}} (\mathbf{D}^n - \mathbf{E}^n) \\ \mathbf{f}_a^{n+1} &= \mathbf{f}_a^n + \frac{\Delta t}{\rho_{sand} L_a} \left[\tilde{\mathbf{D}}^n - \tilde{\mathbf{E}}^n - \mathbf{f}_I^n (\mathbf{D}^n - \mathbf{E}^n) \right]. \end{cases} \quad (24)$$

Since the evolution of the marked sand concentration in the active layer depends, through the interface concentration, also on the exchange of sediments with the substrate, it is necessary to store the marked sand concentration in the substrate $f_b(x, z)$ during the simulation. Assuming that at all times $H_{min} < h < H_{max}$, we consider a subdivision of the vertical domain $z \in [H_{min}, H_{max}]$ in N_z intervals of equal size Δz . The midpoints $z_i = H_{min} + (i - 0.5)\Delta z$, $i = 1, \dots, N_z$ are the discretization points of the vertical domain. The whole domain $[0, L] \times [H_{min}, H_{max}]$ is therefore discretized in $N_x \times N_z$ rectangular cells where (x_i, z_j) are the coordinates of the center points. The substrate concentration is constant in each cell and its values are stored in a matrix \mathbf{F}_b such that $[\mathbf{F}_b]_{ij} \simeq f_b(x_i, z_j)$. During evolution, in the zones characterized by net erosion of sediments the interface concentration \mathbf{f}_I is the substrate concentration \mathbf{F}_b in the cell crossed by the interface. In the zones characterized by net deposition the interface concentration \mathbf{f}_I is the concentration in the active layer \mathbf{f}_a , and the substrate concentration in the cells crossed by the interface has to be updated according to the scheme represented in Figure 6 because they incorporate new sediments from the active layer.

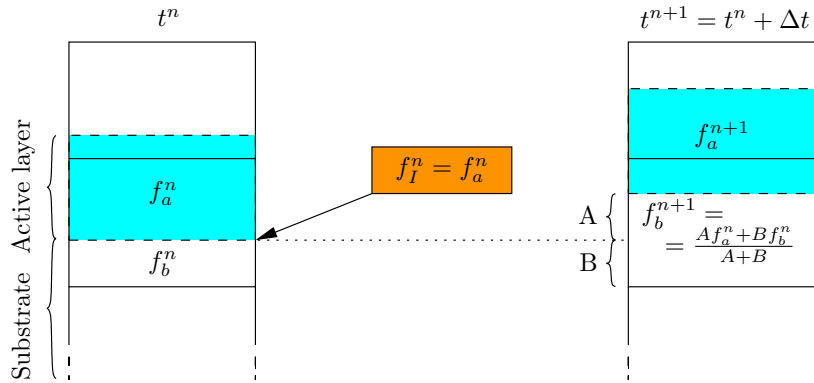


Figure 6: Numerical technique for the passage of sediment from the active layer to the substrate in the case of net deposition.

Sand avalanches First we analyse the entrainment-deposition model for the sand avalanches (21)-(23). The absolute value of the slope in equation (22) is approximated with the finite difference scheme:

$$|\partial_x h| \simeq \frac{1}{\Delta x} \max(h_i - h_{i-1}, h_i - h_{i+1}, 0),$$

which is valid for both positive and negative slopes. As convergence criterion, we iterate the equation (21) until the maximum slope excess is below $tol = 10^{-3}$. Figure 7 shows the relaxation of a steep slope obtained by this algorithm. Here we have considered a domain $x \in [0, 2]$ m subdivided in 200 equally spaced cells of width $\Delta x = 1$ cm and an initial sand pile with surface profile: $h(x, 0) = \max(\cos(\frac{\pi}{2}x), 0)$, which clearly exceeds the maximum admitted slope. In Figure 7 we represent the relaxed surfaces obtained using three different exponential p.d.f. $s_{av}(r)$ with mean equal to 5, 10 and 20 cm; we see that the proposed method effectively relaxes the sand pile. In the same plot we also show the relaxed surface obtained by the algorithm described in Section 2.4; we can note that augmenting the mean step length leads to a tail of the profile at the foot of the relaxed sand pile.

We now couple the discretized active layer model for the evolution of marked

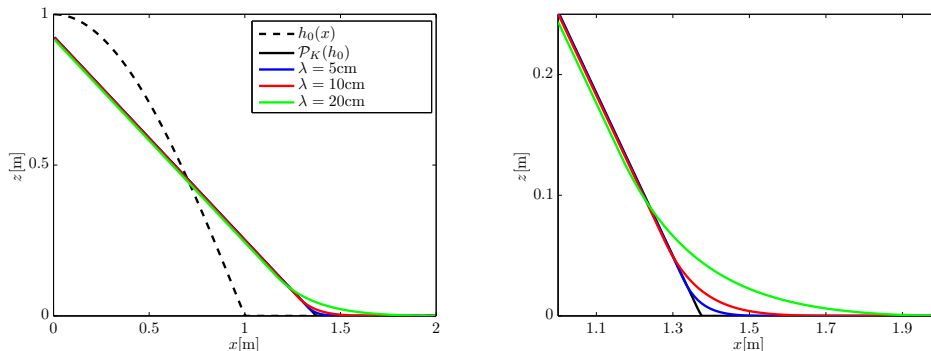


Figure 7: The initial profile $h_0(x)$, (dashed black line) exceeds the maximum admitted slope. The relaxed solution $\mathcal{P}_K(h_0)$ (black line) is approximated (left image) using the entrainment-deposition model for sand avalanches with 3 exponential p.d.f. of rolling grain ($\lambda = 5, 10$ and 20 cm). Zooming at the foot of the sandpile (right image), we see the tail effect which increases with λ .

sand concentration (24) with the model of sand avalanches (assuming that no saltation flux is present). Starting with the discretized domain and the surface profile of the previous example, we discretize the vertical domain $z \in [-0.1, 1.2]$ m in 130 intervals of height $\Delta z = 1$ cm. On this domain, we initialize the marked sand concentrations to the values $f_a(x) = f_b(x, y) = 1 - x$, as represented in Figure 8(a). We use an exponential p.d.f. $s_{av}(r)$ for rolling grains with mean $\lambda = 5$ cm, and define the width of the active layer $L_a = 2.5$ mm,

equal to 10 times the diameter of a sand grain. In Figure 8(b) we can note that the model reproduces a reasonable final sedimentary structure of the collapsed sandpile. In the final solution, the deeper layers of final sedimentary structure are made with sand which comes from the lower part of the initial sandpile, and this is noticeable by a lower concentration of marked sand. On the contrary, the upper layers of the collapsed sandpile come from the upper part of the initial sandpile.

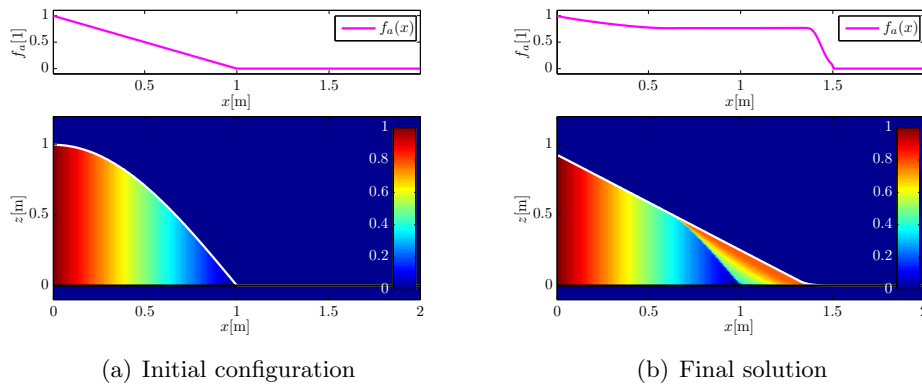


Figure 8: Simulation of the active layer model coupled with the avalanche model. In the upper part is reported the profile of the marked sand concentration in the active layer \mathbf{f}_a , in the lower part the concentration of marked sand in the substrate \mathbf{F}_b .

Dune collision We now propose an application of the model of dune evolution coupled with marked sand dispersion. We recall that, to simulate the complete model, at each time step of the discretized version of system (20), which describes the model for sand transport in saltation, we iterate the avalanche model (21)-(23) until convergence is reached. We consider the domain $[0, 200] \times [-0.5, 5.5]$ discretized with 500×120 cells of $\Delta x = 40$ cm, $\Delta z = 5$ cm. We consider an input wind intensity $U_* = 0.5$ m/s on an initial surface formed by two symmetric bumps of sand, the first 20 m wide and 2 m high, the second 40 m wide and 4 m high. The volume ratio between the two initial bumps is chosen such that the two dunes collide forming a single dune [20]. It is interesting to study how the sand of the first dune redistributes during the collision. For this purpose, we assume that initially the smallest dune is formed by marked sand.

Two consideration must be made regarding the numerical implementation of our model in the case of a large domain: first, as the considered Δx are $> 10^{-1}$ m, the p.d.f. for the step length of avalanching grain considered in the previous examples are not able to reproduce the avalanche in a reasonable number of iterations; the numerical experiments that we performed demonstrate that a good choice is to take $s_{av}(r) = \delta(\Delta x)$, that is all the sand that we entrain from

one cell is deposited on the cell aside. Second, the choice of the parameter L_a limit the choice of the Δt to use in (24), for stability reasons. Since the time scales required to observe dune movement are of the order of $10^1 - 10^3$ days, we have taken a (large) value for L_a to limit the overall computational cost. In particular, we have chosen $L_a = 25$ mm (100 sand grain diameter) and $\Delta t = 6$ min, which is a quite reasonable value for the time scales considered. With these choices of the parameters, the evolution of the model is represented in Figure 9, where we can note the evolution of the marked sand concentration during the collision. At the end, a big dune with marked sand concentration $\simeq 0.2$ (that is the initial volume ratio of marked sand in the simulation) is formed.

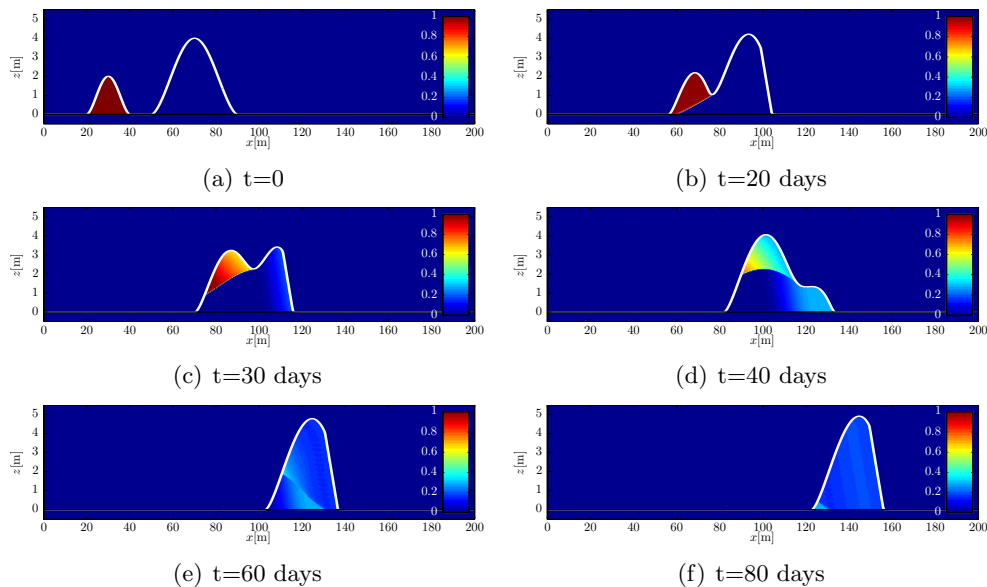


Figure 9: Dune collision: as initial condition, the first smaller dune is made of marked sand; as it's faster than the bigger, the two dune collides. At different time step, we see the marked sand concentration during dune collision.

4 Conclusions

In this work we have first reviewed a simple model for two dimensional dune evolution. We have detailed our original numerical discretization of the system of equation, as we have noticed that this topic is often omitted in the works proposed in the aeolian community. Then we have introduced a mathematical model for marked sand dispersion, based on the active layer hypothesis and on the entrainment-deposition formulation. These two models have already been introduced in the fluvial literature. In this work we applied such theoretical framework to the aeolian case by providing some coherent constitutive relationship for the entrainment rate and for the p.d.f. for step length. Of course the

proposed formulation needs to be supported by theoretical evidences and validated through experimental campaign (in field and wind tunnel) for tracers sediment dispersion; notwithstanding, we think that our work may constitute a starting point for the study of some interesting problems such as dune collision and sand tracking with a new modelling framework.

References

- [1] K. Kroy, G. Sauermann, and H. J. Herrmann, Minimal model for aeolian sand dunes, *Physical Review E*, vol. 66, no. 3, p. 031302, 2002.
- [2] G. Sauermann, K. Kroy, and H. Herrmann, Continuum saltation model for sand dunes, *Physical Review E*, vol. 64, no. 3, p. 031305, 2001.
- [3] V. Schwämmle and H. Herrmann, Modelling transverse dunes, *Earth Surface Processes and Landforms*, vol. 29, no. 6, pp. 769–784, 2004.
- [4] V. Schwämmle and H. Herrmann, A model of barchan dunes including lateral shear stress, *The European Physical Journal E: Soft Matter and Biological Physics*, vol. 16, no. 1, pp. 57–65, 2005.
- [5] P. Hersen, On the crescentic shape of barchan dunes, *The European Physical Journal B-Condensed Matter and Complex Systems*, vol. 37, no. 4, pp. 507–514, 2004.
- [6] E. Parteli, O. Durán, H. Tsoar, V. Schwämmle, and H. Herrmann, Dune formation under bimodal winds, *Proceedings of the National Academy of Sciences*, vol. 106, no. 52, p. 22085, 2009.
- [7] O. Durán, E. J. Parteli, and H. J. Herrmann, A continuous model for sand dunes: Review, new developments and application to barchan dunes and barchan dune fields, *Earth Surface Processes and Landforms*, vol. 35, no. 13, pp. 1591–1600, 2010.
- [8] B. Willetts *et al.*, Particle dislodgement from a flat sand bed by wind, *Earth Surface Processes and Landforms*, vol. 13, no. 8, pp. 717–728, 1988.
- [9] L. Cabrera and I. Alonso, Correlation of aeolian sediment transport measured by sand traps and fluorescent tracers, *Journal of Marine Systems*, vol. 80, no. 3-4, pp. 235–242, 2010.
- [10] G. Parker, Selective sorting and abrasion of river gravel. I. Theory, *Journal of Hydraulic Engineering*, vol. 117, no. 2, pp. 131–149, 1991.
- [11] G. Parker, C. Paola, and S. Leclair, Probabilistic Exner sediment continuity equation for mixtures with no active layer, *Journal of Hydraulic Engineering*, vol. 126, p. 818, 2000.

- [12] P. Jackson and J. Hunt, Turbulent wind flow over a low hill, *Quarterly Journal of the Royal Meteorological Society*, vol. 101, no. 430, pp. 929–955, 1975.
- [13] B. Andreotti, P. Claudin, and S. Douady, Selection of dune shapes and velocities part 1: Dynamics of sand, wind and barchans, *The European Physical Journal B*, vol. 28, no. 3, pp. 321–339, 2002.
- [14] B. Andreotti, P. Claudin, and S. Douady, Selection of dune shapes and velocities part 2: A two dimensional modelling, *The European Physical Journal B*, vol. 28, no. 3, pp. 341–352, 2002.
- [15] R. Bagnold, *The physics of blown sand and desert dunes*. Chapman and Hall, London, 1941.
- [16] B. Andreotti, P. Claudin, and O. Pouliquen, Measurements of the aeolian sand transport saturation length, *Geomorphology*, vol. 123, no. 3-4, pp. 343 – 348, 2010.
- [17] C. Shu, High order weighted essentially non-oscillatory schemes for convection dominated problems, *SIAM review*, vol. 51, no. 1, pp. 82–126, 2009.
- [18] A. Caboussat and R. Glowinski, A numerical method for a non-smooth advection-diffusion problem arising in sand mechanics, *Commun. Pure Appl. Anal*, vol. 8, no. 1, pp. 161–178, 2009.
- [19] V. Ganti, M. Meerschaert, E. Foufoula-Georgiou, E. Viparelli, and G. Parker, Normal and anomalous diffusion of gravel tracer particles in rivers, *Journal of Geophysical Research. F. Earth Surface*, vol. 115, 2010.
- [20] S. Diniega, K. Glasner, and S. Byrne, Long-time evolution of models of aeolian sand dune fields: Influence of dune formation and collision, *Geomorphology*, vol. 121, no. 1-2, pp. 55–68, 2010.

MOX Technical Reports, last issues

Dipartimento di Matematica “F. Brioschi”,
Politecnico di Milano, Via Bonardi 9 - 20133 Milano (Italy)

- 28/2011** PISCHIUTTA, M.; FORMAGGIA, L.; NOBILE, F.
Mathematical modelling for the evolution of aeolian dunes formed by a mixture of sands: entrainment-deposition formulation
- 27/2011** ANTONIETTI, P.F.; BIGONI, N.; VERANI, M.
A Mimetic Discretization of Elliptic Control Problems
- 26/2011** SECCHI, P.; VANTINI, S.; VITELLI, V.
Bagging Voronoi classifiers for clustering spatial functional data
- 25/2011** DE LUCA, M.; AMBROSI, D.; ROBERTSON, A.M.; VENEZIANI, A.; QUARTERONI, A.
Finite element analysis for a multi-mechanism damage model of cerebral arterial tissue
- 24/2011** MANZONI, A.; QUARTERONI, A.; ROZZA, G.
Model reduction techniques for fast blood flow simulation in parametrized geometries
- 23/2011** BECK, J.; NOBILE, F.; TAMELLINI, L.; TEMPONE, R.
On the optimal polynomial approximation of stochastic PDEs by Galerkin and Collocation methods
- 22/2011** AZZIMONTI, L.; IEVA, F.; PAGANONI, A.M.
Nonlinear nonparametric mixed-effects models for unsupervised classification
- 21/2011** AMBROSI, D.; PEZZUTO, S.
Active stress vs. active strain in mechanobiology: constitutive issues
- 20/2011** ANTONIETTI, P.F.; HOUSTON, P.
Preconditioning high-order Discontinuous Galerkin discretizations of elliptic problems
- 19/2011** PASSERINI, T.; SANGALLI, L.; VANTINI, S.; PICCINELLI, M.; BACIGALUPPI, S.; ANTIGA, L.; BOCCARDI, E.; SECCHI, P.; VENEZIANI, A.
An Integrated Statistical Investigation of the Internal Carotid Arteries hosting Cerebral Aneurysms